

Published in final edited form as:

*Cell Metab.* 2013 March 5; 17(3): 343–352. doi:10.1016/j.cmet.2013.01.013.

## Snx3 regulates recycling of the transferrin receptor and iron assimilation

Caiyong Chen<sup>1</sup>, Daniel Garcia-Santos<sup>2,§</sup>, Yuichi Ishikawa<sup>1,§</sup>, Alexandra Seguin<sup>3</sup>, Liangtao Li<sup>3</sup>, Katherine H. Fegan<sup>4</sup>, Gordon J. Hildick-Smith<sup>1</sup>, Dhvanit I. Shah<sup>1</sup>, Jeffrey D. Cooney<sup>1,†</sup>, Wen Chen<sup>1,†</sup>, Matthew J. King<sup>1</sup>, Yvette Y. Yien<sup>1</sup>, Iman J. Schultz<sup>1,†</sup>, Heidi Anderson<sup>1,†</sup>, Arthur J. Dalton<sup>1</sup>, Matthew L. Freedman<sup>5</sup>, Paul D. Kingsley<sup>4</sup>, James Palis<sup>4</sup>, Shilpa M. Hattangadi<sup>6,7,8,†</sup>, Harvey F. Lodish<sup>7</sup>, Diane M. Ward<sup>3</sup>, Jerry Kaplan<sup>3</sup>, Takahiro Maeda<sup>1</sup>, Prem Ponka<sup>2</sup>, and Barry H. Paw<sup>1,6,8,\*</sup>

<sup>1</sup>Department of Medicine, Division of Hematology, Brigham and Women's Hospital, Harvard Medical School, Boston, Massachusetts 02115, USA

<sup>2</sup>Lady Davis Institute for Medical Research, Jewish General Hospital and Department of, Physiology, McGill University, Montreal, Quebec, H3G 1Y6, Canada

<sup>3</sup>Department of Pathology, University of Utah School of Medicine, Salt Lake City, Utah 84312, USA

<sup>4</sup>Department of Pediatrics, Center for Pediatric Biomedical Research, University of Rochester, School of Medicine and Dentistry, Rochester, New York 14642, US

<sup>5</sup>Department of Medical Oncology, Dana-Farber Cancer Institute, Harvard Medical School, Boston, Massachusetts 02115, USA

<sup>6</sup>Department of Medicine, Division of Hematology-Oncology, Boston Children's Hospital, Harvard Medical School, Boston, Massachusetts 02115, USA

<sup>7</sup>Whitehead Institute for Biomedical Research and Massachusetts Institute of Technology, Cambridge, Massachusetts 02142, USA

© 2013 Elsevier Inc. All rights reserved.

Correspondence and requests for materials should be addressed to B.H.P. (bpaw@rics.bwh.harvard.edu).

<sup>§</sup>Equal contributions

<sup>†</sup>Present addresses: University of Texas Health Science Center, San Antonio, Texas 78229, USA (J.D.C.); Texas A&M Health Science Center, Temple, Texas 76504, USA (W.C.); InteRNA Technologies, 3584 CH Utrecht, The Netherlands (I.J.S.); University of Helsinki, 00014 Helsinki, Finland (H.A.); Yale University School of Medicine, New Haven, Connecticut 06510, USA (S.M.H.).

Supplemental information. Supplemental Information includes 7 figures, 1 table, Supplemental Experimental Procedures, and Supplemental References.

**Author Contributions.** C.C. and B.H.P. designed studies, performed experiments, analyzed data, and wrote the manuscript. D.G. and P.P. measured the uptake of <sup>59</sup>Fe-Tf. Y.I. and T.M. measured the surface-bound Tfrc level and the recycling of internalized Tf-Alexa 647. A.S., L.L., D.M.W., and J.K. analyzed the subcellular localization of Tf-Alexa 488 and performed the enzymatic assays. K.H.F., P.D.K., and J.P. performed the in situ hybridization studies in mouse embryos. G.J.H-S. and J.D.C. performed flow cytometry experiments on *Tg(globin-LCR:eGFP)* line. D.I.S. performed the qRT-PCR analysis. W.C. constructed Tfrc-FLAG and Abcb10-FLAG constructs and generated the MEL clones stably expressing these constructs. M.J.K., Y.Y., I.J.S., H.A., and A.J.D. helped with RNA-seq data analysis and zebrafish colony maintenance. M.F. analyzed the GWAS database for potential interesting SNPs in *Snx3*. S.M.H. and H.F.L. provided gene expression data from the RNA-seq experiment and knocked down *Snx3* in mouse primary fetal liver cells.

The authors declare no competing financial interests.

**Publisher's Disclaimer:** This is a PDF file of an unedited manuscript that has been accepted for publication. As a service to our customers we are providing this early version of the manuscript. The manuscript will undergo copyediting, typesetting, and review of the resulting proof before it is published in its final citable form. Please note that during the production process errors may be discovered which could affect the content, and all legal disclaimers that apply to the journal pertain.

<sup>8</sup>Department of Pediatric Oncology, Dana-Farber Cancer Institute, Harvard Medical School, Boston, Massachusetts 02115, USA

## SUMMARY

Sorting of endocytic ligands and receptors is critical for diverse cellular processes. The physiological significance of endosomal sorting proteins in vertebrates, however, remains largely unknown. Here we report that sorting nexin 3 (Snx3) facilitates the recycling of transferrin receptor (Tfrc), and thus is required for the proper delivery of iron to erythroid progenitors. *Snx3* is highly expressed in vertebrate hematopoietic tissues. Silencing of *Snx3* results in anemia and hemoglobin defects in vertebrates due to impaired transferrin (Tf)-mediated iron uptake and its accumulation in early endosomes. This impaired iron assimilation can be complemented with non-Tf iron chelates. We show that Snx3 and Vps35, a component of the retromer, interact with Tfrc to sort it to the recycling endosomes. Our findings uncover a role of Snx3 in regulating Tfrc recycling, iron homeostasis, and erythropoiesis. Thus, the identification of Snx3 provides a genetic tool for exploring erythropoiesis and disorders of iron metabolism.

## INTRODUCTION

Iron is an essential cofactor in diverse biological processes such as oxygen transport, electron transport, signal transduction, and DNA synthesis. In mammals, extraintestinal cells such as developing erythrocytes primarily depend on the transferrin (Tf) cycle to acquire iron from the circulation (Andrews, 2008; Hentze et al., 2004; Levy et al., 1999). Each Tf can bind two ferric iron (Fe<sup>3+</sup>) molecules. The diferric Tf may interact with transferrin receptor (Tfrc) on the cell surface, followed by internalization through clathrin-mediated endocytosis. During the acidification and maturation of endosomes, iron is reduced by six-transmembrane epithelial antigen of the prostate member 3 (Steap3) and subsequently exported out of endosomes by divalent metal transporter 1 (Fleming et al., 1998; Gunshin et al., 1997; Ohgami et al., 2005). This iron may either be delivered to the cytoplasmic iron storage protein ferritin or iron-containing enzymes by poly (rC) binding proteins (Nandal et al., 2011; Shi et al., 2008), or be imported into the mitochondria for the synthesis of heme and iron sulfur clusters by mitoferrin 1 (Mfrn1, Slc25a37) and its partner Abcb10 in developing erythroblasts (Chen et al., 2009; Shaw et al., 2006). The rest of the Tf complex, apo-Tf and Tfrc, are sorted into the recycling endosomes and returned to the cell surface.

The Tf cycle involves three major processes in Tf-Tfrc trafficking: internalization into early endosomes, sorting into recycling endosomes, and recycling to the cell surface (Chen and Paw, 2012; Schultz et al., 2010). Each of these unidirectional movements is likely to be mediated by specific trafficking machinery. The final step, the trafficking of Tfrc from recycling endosomes to the cell surface, has previously been shown to be mediated by Sec1511, as its mutation causes anemia in the *hemoglobin deficit (hbd)* mouse (Lim et al., 2005; White et al., 2005; Zhang et al., 2006). The sorting mechanisms responsible for earlier trafficking events in the Tf cycle, however, remain poorly understood.

Sorting nexins (Snxs) are a family of phosphoinositide-binding proteins that play critical roles in many cellular pathways including nutrient uptake, signal transduction, and development (Cullen and Korswagen, 2012; Johannes and Popoff, 2008). They are essential components of retromer complexes that regulate the retrograde protein transport through early endosomes. The classical retromer complex is composed of the cargo-selective component, Vps26-Vps29-Vps35, and a heterodimeric coat formed by Snx1, Snx2, Snx5, and Snx6 (Cullen and Korswagen, 2012; Johannes and Popoff, 2008; Johannes and Wunder, 2011). Besides these four sorting nexin members, mammals have 29 additional Snxs (Cullen, 2008). These Snxs may have evolved more specialized functions and may regulate

retrograde trafficking in tissue-specific or cargo-selective manners. *In vitro* cell biological studies have implicated several Snxs, including Snx4, Snx9, Snx15, and Snx18, in regulating Tf uptake and Tfrc internalization (Barr et al., 2000; Park et al., 2010; Traer et al., 2007); however, direct evidence is lacking regarding the functional significance of these molecules in mammalian iron physiology.

From an mRNA sequencing experiment, we found that *Snx3* is highly expressed in developing red cells and hematopoietic tissues. Given the intriguing role of the Snx family members in intracellular trafficking along with the strong induction of *Snx3* during erythroid maturation, we hypothesized a functional role for Snx3 in Tf-mediated iron metabolism. To dissect the biochemical function of Snx3 in red cell development, we utilized loss-of-function studies in zebrafish embryos and mammalian erythroid cells. Our complementary results from genetic, biochemical, and biological studies consistently show that Snx3 regulates Tfrc trafficking and is essential for maintaining vertebrate iron homeostasis.

## RESULTS

### *Snx3* is highly expressed in erythroid tissues

Since maturing erythroblasts consume a large amount of iron for the production of heme and hemoglobin (Andrews, 2008; Richardson et al., 2010), it is likely that the sorting molecules responsible for Tf-mediated iron uptake would be abundantly expressed in erythroid tissues. To identify candidate trafficking genes involved in erythropoiesis, we analyzed gene expression profiles during red cell differentiation from an mRNA sequencing (RNA-seq) experiment (Wong et al., 2011). Cells from mouse fetal liver, an organ for definitive erythropoiesis, were sorted by flow cytometry into five distinct sub-populations (R1 to R5), reflecting progressive stages of erythroid maturation (Zhang et al., 2003). We found that the expression of an endosomal sorting molecule, *Snx3*, was up-regulated >3.5 fold in all later stages of differentiating erythroblasts relative to primitive progenitor cells (Figure 1A). The expression profile of *Snx3* is similar to that of *Tfrc* and heme synthesis genes such as *ferrochelatase* (*Fech*), suggesting that they may have coordinated functions. In contrast, no substantial changes in the expression were observed for the genes encoding classical retromer components (Table S1). In worms and flies, SNX3 has been shown to control Wnt signaling by regulating the retromer-dependent transport of Wntless, a membrane protein required for Wnt secretion (Harterink et al., 2011; Zhang et al., 2011). Cell biological studies in human epidermoid carcinoma cells suggest that SNX3 controls endosomal morphology and endocytic cargo transport (Xu et al., 2001). However, the role of Snx3 in iron homeostasis and vertebrate erythropoiesis is unknown.

To confirm the enriched expression of *Snx3* and thus its potential function in hematopoietic tissues, we examined the expression pattern of *Snx3* in developing mouse embryos. Consistent with the RNA-seq data, *Snx3* was highly expressed in mouse primitive (yolk sac at E8.5) and definitive hematopoietic tissues (fetal liver at E12.5 and E15.5, Figure 1B). The specificity of *Snx3* signal was confirmed by using a negative control gene, which displayed no staining in the blood islands of mouse embryos (Figure S1). At E15.5, *Snx3* was also expressed in heart, lung, kidney, and gut, suggesting that it may play a role, in either iron metabolism or Wnt signaling, in these tissues. To further interrogate the erythroid enrichment profile of *Snx3*, we chemically differentiated mouse Friend erythroleukemia (MEL) cells with dimethyl sulfoxide (DMSO), and analyzed their protein levels by western analysis. We found that Snx3, as well as the erythroid proteins, Tfrc and Fech, were induced during MEL cell differentiation (Figures 1C and 1D). The expression pattern of Snx3 closely resembled that of Tfrc. Both proteins displayed increased abundance in the first 4 days and a moderate reduction at day 5, whereas evident up-regulation for Fech was observed between day 3 and day 5 after chemical differentiation, consistent with the

phenomenon that iron acquisition precedes heme synthesis (Figures 1C and 1D). In contrast to *Snx3* and other erythroid genes, *Snx4*, a sorting nexin previously implicated in Tfrc trafficking (Traer et al., 2007), did not show differential expression during erythroid maturation (Figures 1A, 1C, and 1D). This indicates that although *Snx4* was shown to regulate endosomal sorting of Tfrc in HeLa cells (Traer et al., 2007), it may not be the primary sorting molecule that regulates Tf-mediated iron uptake in red cells.

To further examine whether the erythroid expression of *Snx3* is conserved among higher vertebrates, we performed whole mount *in situ* hybridization (WISH) analysis on zebrafish embryos. We detected robust expression of *snx3* in the intermediate cell mass (ICM), the functional equivalent tissue of the yolk sac blood islands in mammals, in a pattern similar to the erythroid transcription factor *gata1* (Figure 2A). The ICM expression for *snx3* was further verified using *cloche*, a mutant lacking hematopoietic stem cells and vascular progenitors (Stainier et al., 1995), and *dino*, a mutant with expanded blood due to its ventralized phenotype (Hammerschmidt et al., 1996). Similar to the erythroid markers *tfr1a* and *gata1*, zygotic expression of *snx3* was first detected in the ICM between 10 and 15-somite stages in zebrafish embryos (Figure S2A). Taken together, our data consistently show that the expression of *Snx3* is enriched in erythroid tissues of higher vertebrates.

### Morpholino knockdown of *snx3* produces anemia in zebrafish

To elucidate the role of *Snx3* in erythropoiesis, we knocked down *snx3* in zebrafish embryos with a translation-blocking morpholino and a pre-mRNA splice-blocking morpholino (Figure S2B). Results from reverse transcription PCR (RT-PCR) validated that the injection of the splice-blocking morpholino interfered with the splicing of *snx3* pre-mRNA (Figure S2C). Western analysis revealed that both morpholinos specifically reduced the expression of *snx3*, while the controls, *snx4* and  $\alpha$ -actin, were unaffected (Figure 2B). Knockdown of *snx3* in zebrafish embryos resulted in a profound anemia, as indicated by the absence of  $\alpha$ -dianisidine positive hemoglobinized cells, at both 48 and 72 hours post fertilization (hpf) (Figure 2C). To determine whether the anemic phenotype was due to impaired heme production or a defect in hematopoiesis, we examined the expression of an erythroid progenitor marker (*gata1*), a terminal erythroid marker ( *$\beta$ e1 globin*), and a myeloid lineage marker (myeloperoxidase, *mpo*). The expression of both *gata1* and *mpo* was normal in *snx3*-deficient embryos (Figure S2D), indicating that neither erythroid nor myeloid specification was affected. We detected robust expression of  *$\beta$ e1 globin* in *snx3*-morphant embryos at 48 hpf despite the absence of heme staining (Figures 2C and S2E), suggesting that these *globin*-expressing erythrocytes are hypochromic. The morphant embryos, however, exhibited substantial decreases in the red cell numbers at 72 hpf (Figure S2E). We confirmed the reduction in erythrocyte number by silencing *snx3* in a *Tg(globin-LCR:eGFP)* transgenic line, which expresses *gfp* under the *globin* locus control region (LCR) enhancer (Ganis et al., 2012). Quantification by flow cytometry revealed a significant reduction in erythrocytes at 72 hpf, while no change in erythroid cell number was observed at 48 hpf (Figure 2D), confirming the hypochromic anemia at 48 hpf. The decrease in erythroid cell number at the later stage is likely an outcome of apoptosis due to severe iron deficiency. A similar trend in the expression of  *$\beta$ e1 globin* has been observed in the zebrafish mutant *chianti*, which has a *tfr1a* defect (Wingert et al., 2004). These results indicate that *snx3* is required for hemoglobin synthesis in the erythroid tissues of teleosts.

### Silencing of *Snx3* results in hemoglobinization defects in mouse hematopoietic cells

To analyze whether *Snx3* has a conserved role in mammalian red cell development, we silenced *Snx3* in mouse primary fetal liver (MPFL) cells using shRNA hairpins (Figure 3A). Consistent with the results in zebrafish, retroviral infection of *Snx3* shRNAs resulted in >75% reduction in total hemoglobin content (Figure 3B). To further understand the

erythroid function of *Snx3*, we generated two stable MEL cell clones expressing *Snx3*-shRNAs. Under both undifferentiated and chemically differentiated conditions, *Snx3* expression was efficiently silenced (Figure 3C). The expression of *Snx4* was not affected, validating the specificity of the targeted knockdown by the shRNAs. Results from  $\alpha$ -dianisidine staining revealed severe defects of hemoglobin production in these *Snx3*-silenced MEL cells (Figures 3D and 3E).

### ***Snx3* is required for cellular iron uptake through regulating the trafficking of Tf-Tfrc complex**

To determine whether the hemoglobinization defect observed in *Snx3*-deficient cells is due to impaired uptake and delivery of Tf-bound iron, we labeled the stable shRNA MEL clones with  $^{59}\text{Fe}$ -saturated Tf. We found a reduction in Tf uptake, iron delivery, as well as iron incorporation into heme in *Snx3*-silenced cells (Figure 4A). Interestingly, these cells have normal activities of iron-containing enzymes such as cytosolic xanthine oxidase and mitochondrial aconitase (Figures S3A and S3B). It is likely that the differentiating erythroid cells may prioritize their limited iron supplies to first fulfill the requirement for the basic cellular processes. In addition, the demand of iron by these processes is much lower than the requirement of iron for heme synthesis in differentiating erythroid cells. When cellular iron is limited, the enzymes involved in basic metabolism such as xanthine oxidase and aconitase may still acquire sufficient amount of iron while less iron is provided for heme production.

To examine whether the reduced iron uptake is due to defective endosomal acidification, a process preceding iron release, we treated the cells with bafilomycin, a specific inhibitor of the vacuolar type H(+)-ATPase (Yoshimori et al., 1991). Treatment with bafilomycin reduced the uptake of  $^{59}\text{Fe}$ -Tf to a similar extent in both control and *Snx3*-silenced cells (Figures 4A and S3C). In the presence of bafilomycin, the *Snx3*-silenced cells still maintained a lower uptake of  $^{59}\text{Fe}$ -Tf than the control cells (Figure 4A), suggesting that this reduced iron uptake is not due to pH alteration in endosomes. In addition, this reduced Tf uptake is not a consequence of decreased accessibility of its receptor, as evidenced by the normal levels of Tfrc on the surface of *Snx3*-silenced cells (Figure 4B).

The reduction in the uptake of Tf iron, despite the presence of the receptor Tfrc, suggests that the *Snx3*-silenced cells may have defective vesicular trafficking of the Tf-Tfrc complex. To characterize the defect in the Tf cycle, we incubated the stable MEL cells with Tf-Alexa 488 and analyzed the subcellular distribution of Tf. We found that in *Snx3*-silenced cells, the Alexa-labeled Tf accumulated as large intracellular clusters (Figures 4C, 4D, S3D, and S3E). The clustered Tf signal colocalized with Tfrc as well as Rab5, a marker for the early endosomal compartment, indicating that the internalized Tf complex is trapped in the enlarged early endosomal compartments. In the majority of control cells, no clustered pattern is observed, indicating constant recycling and clearance of the internalized Tf. These results suggest that the endosomal trafficking of Tf is impaired in *Snx3*-silenced cells.

To quantify the defect on the sorting and recycling of Tf, we pulsed-labeled the *Snx3*-silenced cells with holo-Tf conjugated with fluorescent Alexa 647, and measured the kinetics of Tf release following the chase with unlabeled Tf. As shown in Figure 4E, silencing of *Snx3* significantly delayed the recycling of internalized Tf. The  $t_{1/2}$  of Tf release was >30% longer in the *Snx3*-silenced cells ( $9.99 \pm 0.34$  min and  $10.08 \pm 0.68$  min for the two shRNA clones) than that in the control clone ( $7.36 \pm 0.4$  min). These data indicate that *Snx3* is required for the efficient recycling of Tf-Tfrc complex.



### Silencing of *Snx3* reduces the turnover rate of *Tfrc*

Previously, it was observed that suppression of *Tfrc* recycling accelerated its degradation by lysosomes in HeLa cells (Traer et al., 2007). Is the *Tfrc* accumulated in the early endosomes of *Snx3*-silenced cells more likely to be degraded? Is *Tfrc* expression altered in response to potential changes in its stability as well as cellular iron deficiency in these cells? To address these questions, we rigorously examined the steady state level, the synthesis rate, and the degradation rate of *Tfrc* protein. Results from immunoblotting analysis revealed a moderate decrease in *Tfrc* protein abundance in *Snx3*-silenced clones, suggesting reduced *Tfrc* expression (Figures 5A and 5B). Consistent with this observation, the silencing of *Snx3* produced a severe reduction of ~3.8 fold in *Tfrc* mRNA levels in MEL cells (Figure 5C). The *Tfrc* mRNA has five iron regulatory elements (IREs) in its 3' untranslated region (UTR), and iron deficiency would in general induce its expression by stabilizing the mRNA by iron regulatory proteins (IRPs) (Casey et al., 1988). In erythroid cells, however, the *Tfrc* expression is regulated by mechanisms that are independent of the IRE/IRP system (Chan et al., 1994; Ponka and Lok, 1999; Schranzhofer et al., 2006). To confirm the lack of iron-dependent regulation of *Tfrc* expression in differentiated MEL cells, we treated the wild type cells with the iron chelator desferrioxamine (DFO) and analyzed the *Tfrc* expression by qRT-PCR. The results indicated that iron depletion increased the level of *Tfrc* mRNA in undifferentiated MEL cells, but not in differentiated erythroid-like MEL cells (Figure S4). This evidence supports the notion that the reduction in *Tfrc* mRNA in *Snx3*-silencing cells is mediated through an IRE/IRP-independent mechanism.

To rigorously analyze the effect of *Snx3* deficiency on the synthesis and stability of *Tfrc* protein, we metabolically labeled the cells with L-[<sup>35</sup>S]methionine and L-[<sup>35</sup>S]cysteine and examined the protein turnover rates of *Tfrc*. Consistent with the qRT-PCR data, the stable *Snx3* silenced clones synthesized *Tfrc* protein at a ~3.5fold lower rate than the control (Figures 5D and 5E). In addition, the rate of *Tfrc* degradation following pulse-chase was also lower (~3.1 fold) in *Snx3*-silenced clones (Figures 5D and 5E), suggesting that the *Tfrc* complex accumulated in the endosomal compartments is not missorted into lysosomes for degradation. In contrast to *Tfrc*, the steady state levels of other proteins that traffic through the endosomal compartments, such as Snap23 and Lamp1 (Cook et al., 2004; Valdez et al., 1999), were not significantly altered (Figures S5A and S5B). These results indicate that the abnormal expression and stability of *Tfrc* is not due to a global delay in the progression to lysosomes. Thus, *Snx3*-silenced cells have a reduced turnover rate as well as defective trafficking of *Tfrc*.

### *Snx3* interacts with *Tfrc* in an oligomeric complex

Our findings suggest that when *Tfrc* complex transits through the early endosomes, it may transiently associate with *Snx3* in order to be sorted to the recycling endosomes. To test this hypothesis, we transiently co-expressed *Snx3* and FLAG-tagged *Tfrc* in heterologous HEK293 cells and affinity purified the protein complex associated with *Tfrc* using anti-FLAG beads. The known mitochondrial transmembrane protein Abcb10 was used as a control for nonspecific interactions between membrane-associated proteins (Chen et al., 2009; Shirihai et al., 2000). We detected a significantly higher quantity of *Snx3* that was associated with *Tfrc* than Abcb10 (Figure 6A). To exclude the potential artifact from ectopic over-expression studies, we performed the pull-down assays in MEL cells that stably express either *Tfrc*-FLAG or Abcb10-FLAG driven by the promoter of eukaryotic translation elongation factor 1 $\alpha$ . Under both undifferentiated and DMSO-induced conditions, endogenous *Snx3* specifically interacted with *Tfrc* (Figure 6B). In addition, *Tfrc*, but not Abcb10, was able to pull down Vps35, the cargo-selective component of the retromer complex. These data therefore demonstrate that *Snx3*, together with other retromer

complex components, regulates the endocytic recycling of Tf-Tfrc complex through physical interaction with Tfrc.

### The heme defects due to *Snx3* deficiency are rescued by supplementation with non-Tf bound iron-chelates

To demonstrate the functional specificity of Tfrc-dependent iron uptake pathway affected by *Snx3* deficiency, we tested whether supplementation of non-Tf bound iron-chelates could complement the hemoglobinization defect in *Snx3*-silenced cells and zebrafish embryos. It has been previously reported that iron conjugated with salicylaldehyde isonicotinoyl hydrazone (Fe-SIH) could be taken up by erythroid cells through a Tfrc-independent pathway (Garrick et al., 1991; Zhang et al., 2006). Supplementation of ferric citrate (Fe-citrate), Fe-SIH, or a related chemically-defined iron supplement (Sigma-Aldrich I3153, Fe-chelate mixture, containing EDTA, citrate, and salicylic acid derivative) all increased the population of  $\alpha$ -dianisidine positive cells by 2–5 fold in *Snx3*-silenced MEL clones (Figures 7A and S6). The rescue effects of these iron compounds were further confirmed in zebrafish *in vivo*. Here we took advantage of the observation that *snx3* morphant embryos have reduced number of erythrocytes at 72 hpf, an outcome of apoptosis induced by severe iron deficiency, and rigorously quantified the effects of the non-Tf iron-chelate supplements by flow cytometry (Figure 2D). We found that these iron-chelate supplements increased the number of erythrocytes, as indicated by GFP fluorescence, in *snx3*-silenced *Tg(globin-LCR:eGFP)* embryos (Figure 7B). The gene encoding the mitochondrial iron importer mitoferrin-1 (*slc25a37*), *mfn1*, was used as a control since its knockdown was known to induce hypochromic anemia due to iron deficiency (Shaw et al., 2006). The chemical complementation with the iron-chelate compounds reinforces our proposed model that *Snx3* specifically regulates Tfrc-dependent iron assimilation in red cell development.

## DISCUSSION

Our study demonstrates that *Snx3* regulates endocytic recycling of Tfrc, and thus plays a critical role in cellular iron homeostasis and erythropoiesis in vertebrates (Figure 7C). The yeast homolog of *Snx3*, Grd19p, has been shown to mediate the endocytic recycling of Fet3p-Ftr1p, a yeast-specific reductive iron transporter system, through direct interaction with Ftr1p (Strochlic et al., 2008; Strochlic et al., 2007). Taken together, *Snx3* may play a regulatory role in iron homeostasis across multiple eukaryotic phyla.

*Snx3* is highly expressed in hematopoietic tissues of zebrafish and mouse. To account for the enrichment of *Snx3* mRNA in blood islands and the increase in *Snx3* protein expression in differentiating MEL cells, we searched GATA-1 and EKLF/KLF1 ChIP-seq databases to determine if *Snx3* could be regulated by key transcriptional regulators of erythropoiesis. As predicted, the *Snx3* gene is bound by EKLF/KLF1 (Tallack et al., 2010) and GATA-1 (Yu et al., 2009) *in vivo*. In addition to the regulation at the transcriptional level, the mouse *Snx3* also has a predicted IRE-like structure in the 3' UTR of its mRNA (5'-CGCUGUGUCCGUGUGCACACUG-3') (Campillos et al., 2010). The abundance of *Snx3* mRNA, however, showed no changes in response to either iron depletion with desferrioxamine or iron overload with 200  $\mu$ M ferric citrate (Figure S7), suggesting that the putative IRE is not functional. Furthermore, the putative 3'UTR IRE is not conserved in other vertebrate *Snx3* orthologs.

*Snx3* has been shown to interact with Vps35, the cargo-selective component of retromer (Vardarajan et al., 2012; Zhang et al., 2011). In addition, a proteomic study in yeast detected interactions between Grd19p and Sec15p (Vollert and Uetz, 2004), whose ortholog in mammals was shown to control the sorting of Tf-Tfrc complexes in recycling endosomes (Lim et al., 2005; White et al., 2005; Zhang et al., 2006). Here we found that Tfrc physically

interacts with both Snx3 and Vps35. These data indicate that Snx3 and the Vps proteins may constitute a non-classical retromer complex that interacts with Tf-Tfrc oligomers in early endosomes and deliver them to Sec1511 in recycling endosomes (Figure 7C).

The important role of Snx3 in Tf trafficking was independently validated by studies in mammalian hematopoietic cells. Silencing of *Snx3* reduced the rate of Tf recycling and the uptake of Tf-bound iron (Figures 4A and 4E). In *Snx3*-silenced cells, the internalized Tf accumulated as large intracellular clusters in the early endosomes (Figures 4C and 4D). This defective trafficking may be responsible for the reduced turnover rate of Tfrc protein (Figure 5). Interestingly, although the *Snx3*-silenced cells had an increased level of Tf-Tfrc complexes in the enlarged early endosomes and a reduced amount of total cellular Tfrc, we did not find any reduction in the cell surface-bound Tfrc (Figure 4B). The normal level of Tfrc on the cell surface may be maintained by such factors as the extended stability of Tfrc and the likely reduced internalization rate of Tfrc. The reduced internalization accompanying reduced recycling has been observed for Sec1511, which also plays a regulatory role in the Tf cycle (Zhang et al., 2006). Our data further suggest that the defective Tf trafficking due to *Snx3* deficiency may have altered the distribution of Tfrc between the early and the recycling endosomes, whereas the Tfrc abundance on the cell surface may not be as directly impacted. Further investigation may be needed to test these possibilities and to fully characterize the steady-state equilibrium of Tfrc in the *Snx3*-silenced cells.

In nonerythroid cells, the interaction of Snx3 with Tfrc may be functionally substituted by other receptors, implying a broader role for Snx3 in retromer-mediated vesicular recycling. Two independent reports have shown that Snx3 mediates the retrograde transport of the Wnt sorting receptor Wntless and is required for Wnt secretion in flies and worms (Harterink et al., 2011; Zhang et al., 2011). The involvement of Snx3 in two discrete cellular pathways suggests that it regulates the endosomal sorting of a repertoire of cargo receptors including Tfrc and Wntless, and thus plays a fundamental role in intracellular vesicle trafficking.

The fundamental role of Snx3 in endosomal sorting was further attested by its involvement in the retrograde trafficking of amyloid precursor protein (APP) (Vardarajan et al., 2012). Through analyzing a genome-wide association study (GWAS) dataset, this study identified significant association between the single nucleotide polymorphisms (SNPs) in *SNX3* and Alzheimer disease. Results from this study further indicated that *SNX3* and *VPS* proteins form a retromer complex that mediates the retrieval of APP from endosomes to Golgi, thus preventing the generation of the neurotoxic amyloid  $\beta$  peptide. In addition, another research group located a *SNX3* gene disruption in a patient with microcephaly, microphthalmia, ectrodactyly, and prognathism (MMEP) (Vervoort et al., 2002). However, no mutations in the coding region of *SNX3* were found in five additional patients with MMEP, suggesting that the defect in *SNX3* may not be responsible for the MMEP phenotype (Kumar et al., 2007).

Given the profound anemic phenotype in *snx3*-silenced zebrafish embryos, it is also likely that mutations in *SNX3* may lead to hematological disorders in humans. We therefore searched the NHGRI human GWAS databases (Hindorff et al., 2009), but we were not able to find a significant association between *SNX3* SNPs and the hematologic traits (Ganesh et al., 2009; Soranzo et al., 2009). Two SNPs that are associated with hematologic traits located in the same cytoband as *SNX3*, rs11966072 and rs4947019, are located at a considerable distance (>1 Mb) from the *SNX3* locus, making them unlikely disease causing candidates in *SNX3*. Further genetic and sequencing studies on anemic patients with undefined etiologies may help to reveal the potential connection between *SNX3* and hematological disorders. Thus, the identification of Snx3, as an essential co-regulatory



protein that regulates Tf-mediated iron delivery for heme synthesis, provides a genetic tool for exploring erythropoiesis and human disorders of iron metabolism, such as the hypochromic anemias.

## EXPERIMENTAL PROCEDURES

### Zebrafish Experiments

All zebrafish experiments were performed in compliance with the Institutional Animal Care and Use Committee (IACUC) regulations at Boston Children's Hospital. AB, *cloche* (*clo<sup>m39</sup>*) (Stainier et al., 1995), *dino* (*din<sup>tm84</sup>*) (Hammerschmidt et al., 1996), and *Tg(globin-LCR:eGFP)* (Ganis et al., 2012) transgenic lines were used in this study. Whole-mount *in situ* hybridization was carried out as previously described (Amigo et al., 2011). An ATG-blocking and a splice-blocking anti-sense morpholinos for *snx3* were obtained from Gene Tools (Supplemental Information), and each MO was individually injected into one-cell stage zebrafish embryos. The embryos were harvested at 24~72 hpf for WISH and 48~72 hpf for  $\alpha$ -dianisidine staining, following the protocols described previously (Shaw et al., 2006). Flow cytometry on the *Tg(globin LCR:eGFP)* embryos was performed as previously described (Cooney et al., 2013).

### Knock down of *Snx3* in mouse cells

shRNA constructs (Supplemental Information) were purchased from Sigma-Aldrich. Stable *Snx3*-silenced MEL clones were generated by electroporation, followed by selection with puromycin. *Snx3* was silenced in MPFL cells by infection with retroviruses containing shRNAs for *Snx3* (Hattangadi et al., 2010). The knockdown efficiency was examined by immunoblotting analysis. The hemoglobin in stable MEL cells was stained with  $\alpha$ -dianisidine, and the hemoglobin content in MPFL was measured with Drabkin's reagent (Hattangadi et al., 2010).

### Transferrin uptake and immunofluorescence assays

Stable *Snx3*-silenced MEL clones were labeled with <sup>59</sup>Fe-transferrin as previously described (Zhang et al., 2006). <sup>59</sup>FeCl<sub>3</sub> (specific activity: 42.59 mCi/mg) was obtained from PerkinElmer. The MEL cells were also incubated with transferrin-Alexa 488 followed by immunofluorescence studies using antibodies against Tfrc and Rab5.

### Metabolic [<sup>35</sup>S]-labeling

Stable *Snx3*-silenced MEL cells were labeled with L-[<sup>35</sup>S]methionine and L-[<sup>35</sup>S]cysteine (PerkinElmer, >1,000 Ci/mmol specific activity) following a protocol described previously (Paradkar et al., 2009). The abundance of [<sup>35</sup>S]-labeled Tfrc was examined at different time during both pulse and pulse-chase phases.

### Tfrc pull-down assays

The FLAG-tagged *Tfrc* and *Abcb10* constructs were generated using the same strategy as previously reported (Chen et al., 2009). MEL clones stably expressing *Tfrc-FLAG* or *Abcb10-FLAG* were generated by electroporation followed by puromycin selection. Cell lysates from the stable MEL cells or HEK293 cells transiently transfected with *Snx3* plasmids in combination with *Tfrc-FLAG* or *Abcb10-FLAG* were subjected to FLAG pull-down assays using ANTI-FLAG M2 Affinity Gel (Chen et al., 2009).

### Iron supplementation experiments

A chemically defined iron supplement (Sigma-Aldrich, I3153; EC #231-791-2), 20  $\mu$ M Fe-SIH, or 20  $\mu$ M Fe-citrate was supplemented to MEL cells during the erythroid-like

induction. The embryos from *Tg(globin-LCR:eGFP)* transgenic zebrafish were injected with morpholinos against *srx3* or the positive control *mfn1*. These zebrafish embryos were treated with the chemically defined iron supplement or 10  $\mu$ M Fe-SIH at 30 hpf, and were analyzed for the percentage of erythrocytes based on GFP fluorescence by flow cytometry at 72 hpf.

### Statistical analysis

All data are presented as mean  $\pm$  standard error of the mean (SEM). Statistical significance was tested using one-way ANOVA followed by the Tukey-Kramer Multiple Comparisons Test in GraphPad INSTAT version 3.01 (GraphPad, San Diego, CA, USA). A *P* value of < 0.05 was considered as statistically significant.

### Supplementary Material

Refer to Web version on PubMed Central for supplementary material.

### Acknowledgments

We thank members of our lab (Jacky Chung, Diana Branco, Adrienne Kolpak) and Dr. Elizabeth Leibold for critical discussion and reading of the manuscript, Dr. Yan Zhang for help with the enzymatic assays, Dr. Rebecca Wingert for the zebrafish *tfr1a* cDNA clone, Dr. Leonard Zon for the *Tg(globin LCR:eGFP)* transgenic line, Dr. Karin Hoffmeister for use of the FACS machine, and Christian Lawrence and his team for the zebrafish husbandry. This work was supported by grants from the Cooley's Anemia Foundation (C.C., D.I.S.), the American Heart Association (J.D.C., M.J.K., A.J.D.), the American Society of Hematology (M.J.K.), the Dutch National Science Fund-NWO (I.J.S.), the Finnish Sigrid Juselius Foundation (H.A.), the March of Dimes Foundation (6-FY09-289, B.H.P.), the Canadian Institutes of Health Research (D.S. and P.P.), and the National Institutes of Health (T32 HL007574, Y.Y.Y.; K01 DK085217, D.I.S.; K08 DK076848, S.M.H.; R01 DK09361, J.P.; P01 HL032262, H.F.L.; R01 HL026922, D.M.W.; R01 DK052380, J.K.; R01 DK070838 and P01 HL032262, B.H.P.).

### References

- Amigo JD, Yu M, Troadec MB, Gwynn B, Cooney JD, Lambert AJ, Chi NC, Weiss MJ, Peters LL, Kaplan J, et al. Identification of distal cis-regulatory elements at mouse mitoferrin loci using zebrafish transgenesis. *Mol Cell Biol*. 2011; 31:1344–1356. [PubMed: 21248200]
- Andrews NC. Forging a field: the golden age of iron biology. *Blood*. 2008; 112:219–230. [PubMed: 18606887]
- Barr VA, Phillips SA, Taylor SI, Haft CR. Overexpression of a novel sorting nexin, SNX15, affects endosome morphology and protein trafficking. *Traffic*. 2000; 1:904–916. [PubMed: 11208079]
- Campillos M, Cases I, Hentze MW, Sanchez M. SIREs: searching for iron-responsive elements. *Nucleic Acids Res*. 2010; 38:W360–367. [PubMed: 20460462]
- Casey JL, Hentze MW, Koeller DM, Caughman SW, Rouault TA, Klausner RD, Harford JB. Iron-responsive elements: regulatory RNA sequences that control mRNA levels and translation. *Science*. 1988; 240:924–928. [PubMed: 2452485]
- Chan RY, Seiser C, Schulman HM, Kuhn LC, Ponka P. Regulation of transferrin receptor mRNA expression. Distinct regulatory features in erythroid cells. *Eur J Biochem*. 1994; 220:683–692. [PubMed: 8143723]
- Chen C, Paw BH. Cellular and mitochondrial iron homeostasis in vertebrates. *Biochim Biophys Acta*. 2012; 1823:1459–1467. [PubMed: 22285816]
- Chen W, Paradkar PN, Li L, Pierce EL, Langer NB, Takahashi-Makise N, Hyde BB, Shirihai OS, Ward DM, Kaplan J, et al. Abcb10 physically interacts with mitoferrin-1 (Slc25a37) to enhance its stability and function in the erythroid mitochondria. *Proc Natl Acad Sci USA*. 2009; 106:16263–16268. [PubMed: 19805291]
- Cook NR, Row PE, Davidson HW. Lysosome associated membrane protein 1 (Lamp1) traffics directly from the TGN to early endosomes. *Traffic*. 2004; 5:685–699. [PubMed: 15296493]

- Cooney JD, Hildick-Smith GJ, Shafizadeh E, McBride PF, Carroll KJ, Anderson H, Shaw GC, Tamplin OJ, Branco DS, Dalton AJ, et al. Teleost growth factor independence (*gfi*) genes differentially regulate successive waves of hematopoiesis. *Dev Biol*. 2013; 373:431–441. [PubMed: 22960038]
- Cullen PJ. Endosomal sorting and signalling: an emerging role for sorting nexins. *Nat Rev Mol Cell Biol*. 2008; 9:574–582. [PubMed: 18523436]
- Cullen PJ, Korswagen HC. Sorting nexins provide diversity for retromer-dependent trafficking events. *Nat Cell Biol*. 2012; 14:29–37. [PubMed: 22193161]
- Fleming MD, Romano MA, Su MA, Garrick LM, Garrick MD, Andrews NC. Nramp2 is mutated in the anemic Belgrade (b) rat: evidence of a role for Nramp2 in endosomal iron transport. *Proc Natl Acad Sci USA*. 1998; 95:1148–1153. [PubMed: 9448300]
- Ganesh SK, Zakai NA, van Rooij FJ, Soranzo N, Smith AV, Nalls MA, Chen MH, Kottgen A, Glazer NL, Dehghan A, et al. Multiple loci influence erythrocyte phenotypes in the CHARGE Consortium. *Nat Genet*. 2009; 41:1191–1198. [PubMed: 19862010]
- Ganis JJ, Hsia N, Trompouki E, de Jong JL, DiBiase A, Lambert JS, Jia Z, Sabo PJ, Weaver M, Sandstrom R, et al. Zebrafish globin switching occurs in two developmental stages and is controlled by the LCR. *Dev Biol*. 2012; 366:185–194. [PubMed: 22537494]
- Garrick LM, Gniecko K, Hoke JE, al-Nakeeb A, Ponka P, Garrick MD. Ferric-salicylaldehyde isonicotinoyl hydrazone, a synthetic iron chelate, alleviates defective iron utilization by reticulocytes of the Belgrade rat. *J Cell Physiol*. 1991; 146:460–465. [PubMed: 2022700]
- Gunshin H, Mackenzie B, Berger UV, Gunshin Y, Romero MF, Boron WF, Nussberger S, Gollan JL, Hediger MA. Cloning and characterization of a mammalian proton-coupled metal-ion transporter. *Nature*. 1997; 388:482–488. [PubMed: 9242408]
- Hammerschmidt M, Pelegri F, Mullins MC, Kane DA, van Eeden FJ, Granato M, Brand M, Furutani-Seiki M, Haffter P, Heisenberg CP, et al. *dino* and *mercedes*, two genes regulating dorsal development in the zebrafish embryo. *Development*. 1996; 123:95–102. [PubMed: 9007232]
- Harterink M, Port F, Lorenowicz MJ, McGough IJ, Silhankova M, Betist MC, van Weering JR, van Heesbeen RG, Middelkoop TC, Basler K, et al. A SNX3-dependent retromer pathway mediates retrograde transport of the Wnt sorting receptor Wntless and is required for Wnt secretion. *Nat Cell Biol*. 2011; 13:914–923. [PubMed: 21725319]
- Hattangadi SM, Burke KA, Lodish HF. Homeodomain-interacting protein kinase 2 plays an important role in normal terminal erythroid differentiation. *Blood*. 2010; 115:4853–4861. [PubMed: 20231426]
- Hentze MW, Muckenthaler MU, Andrews NC. Balancing acts: molecular control of mammalian iron metabolism. *Cell*. 2004; 117:285–297. [PubMed: 15109490]
- Hindorf LA, Sethupathy P, Junkins HA, Ramos EM, Mehta JP, Collins FS, Manolio TA. Potential etiologic and functional implications of genome-wide association loci for human diseases and traits. *Proc Natl Acad Sci USA*. 2009; 106:9362–9367. [PubMed: 19474294]
- Johannes L, Popoff V. Tracing the retrograde route in protein trafficking. *Cell*. 2008; 135:1175–1187. [PubMed: 19109890]
- Johannes L, Wunder C. The SNXy flavours of endosomal sorting. *Nat Cell Biol*. 2011; 13:884–886. [PubMed: 21725318]
- Kumar RA, Everman DB, Morgan CT, Slavotinek A, Schwartz CE, Simpson EM. Absence of mutations in NR2E1 and SNX3 in five patients with MMEP (microcephaly, microphthalmia, ectrodactyly, and prognathism) and related phenotypes. *BMC Med Genet*. 2007; 8:48. [PubMed: 17655765]
- Levy JE, Jin O, Fujiwara Y, Kuo F, Andrews NC. Transferrin receptor is necessary for development of erythrocytes and the nervous system. *Nat Genet*. 1999; 21:396–399. [PubMed: 10192390]
- Lim JE, Jin O, Bennett C, Morgan K, Wang F, Trenor CC 3rd, Fleming MD, Andrews NC. A mutation in Sec15l1 causes anemia in hemoglobin deficit (*hbd*) mice. *Nat Genet*. 2005; 37:1270–1273. [PubMed: 16227995]
- Ohgami RS, Campagna DR, Greer EL, Antiochos B, McDonald A, Chen J, Sharp JJ, Fujiwara Y, Barker JE, Fleming MD. Identification of a ferrireductase required for efficient transferrin-dependent iron uptake in erythroid cells. *Nat Genet*. 2005; 37:1264–1269. [PubMed: 16227996]

- Park J, Kim Y, Lee S, Park JJ, Park ZY, Sun W, Kim H, Chang S. SNX18 shares a redundant role with SNX9 and modulates endocytic trafficking at the plasma membrane. *J Cell Sci.* 2010; 123:1742–1750. [PubMed: 20427313]
- Ponka P, Lok CN. The transferrin receptor: role in health and disease. *Int J Biochem Cell Biol.* 1999; 31:1111–1137. [PubMed: 10582342]
- Richardson DR, Lane DJ, Becker EM, Huang ML, Whitnall M, Suryo Rahmanto Y, Sheftel AD, Ponka P. Mitochondrial iron trafficking and the integration of iron metabolism between the mitochondrion and cytosol. *Proc Natl Acad Sci USA.* 2010; 107:10775–10782. [PubMed: 20495089]
- Schranzhofer M, Schiffrer M, Cabrera JA, Kopp S, Chiba P, Beug H, Mullner EW. Remodeling the regulation of iron metabolism during erythroid differentiation to ensure efficient heme biosynthesis. *Blood.* 2006; 107:4159–4167. [PubMed: 16424395]
- Schultz IJ, Chen C, Paw BH, Hamza I. Iron and porphyrin trafficking in heme biogenesis. *J Biol Chem.* 2010; 285:26753–26759. [PubMed: 20522548]
- Shaw GC, Cope JJ, Li L, Corson K, Hersey C, Ackermann GE, Gwynn B, Lambert AJ, Wingert RA, Traver D, et al. Mitoferrin is essential for erythroid iron assimilation. *Nature.* 2006; 440:96–100. [PubMed: 16511496]
- Shirihai OS, Gregory T, Yu C, Orkin SH, Weiss MJ. ABC-me: a novel mitochondrial transporter induced by GATA-1 during erythroid differentiation. *EMBO J.* 2000; 19:2492–2502. [PubMed: 10835348]
- Soranzo N, Spector TD, Mangino M, Kuhnel B, Rendon A, Teumer A, Willenborg C, Wright B, Chen L, Li M, et al. A genome-wide meta-analysis identifies 22 loci associated with eight hematological parameters in the HaemGen consortium. *Nat Genet.* 2009; 41:1182–1190. [PubMed: 19820697]
- Stainier DY, Weinstein BM, Detrich HW 3rd, Zon LI, Fishman MC. Cloche, an early acting zebrafish gene, is required by both the endothelial and hematopoietic lineages. *Development.* 1995; 121:3141–3150. [PubMed: 7588049]
- Strohlic TI, Schmiedekamp BC, Lee J, Katzmann DJ, Burd CG. Opposing activities of the Snx3-retromer complex and ESCRT proteins mediate regulated cargo sorting at a common endosome. *Mol Biol Cell.* 2008; 19:4694–4706. [PubMed: 18768754]
- Strohlic TI, Setty TG, Sitaram A, Burd CG. Grd19/Snx3p functions as a cargo-specific adapter for retromer-dependent endocytic recycling. *J Cell Biol.* 2007; 177:115–125. [PubMed: 17420293]
- Tallack MR, Whittington T, Yuen WS, Wainwright EN, Keys JR, Gardiner BB, Nourbakhsh E, Cloonan N, Grimmond SM, Bailey TL, et al. A global role for KLF1 in erythropoiesis revealed by ChIP-seq in primary erythroid cells. *Genome Res.* 2010; 20:1052–1063. [PubMed: 20508144]
- Traer CJ, Rutherford AC, Palmer KJ, Wassmer T, Oakley J, Attar N, Carlton JG, Kremerskothen J, Stephens DJ, Cullen PJ. SNX4 coordinates endosomal sorting of TfR with dynein-mediated transport into the endocytic recycling compartment. *Nat Cell Biol.* 2007; 9:1370–1380. [PubMed: 17994011]
- Valdez AC, Cabaniols JP, Brown MJ, Roche PA. Syntaxin 11 is associated with SNAP-23 on late endosomes and the trans-Golgi network. *J Cell Sci.* 1999; 112(Pt 6):845–854. [PubMed: 10036234]
- Vardarajan BN, Bruesegem SY, Harbour ME, St George-Hyslop P, Seaman MN, Farrer LA. Identification of Alzheimer disease-associated variants in genes that regulate retromer function. *Neurobiol Aging.* 2012; 33:2231 e2215–2231 e2230. [PubMed: 22673115]
- Vervoort VS, Viljoen D, Smart R, Suthers G, DuPont BR, Abbott A, Schwartz CE. Sorting nexin 3 (SNX3) is disrupted in a patient with a translocation t(6;13)(q21;q12) and microcephaly, microphthalmia, ectrodactyly, prognathism (MMEP) phenotype. *J Med Genet.* 2002; 39:893–899. [PubMed: 12471201]
- Vollert CS, Uetz P. The phox homology (PX) domain protein interaction network in yeast. *Mol Cell Proteomics.* 2004; 3:1053–1064. [PubMed: 15263065]
- White RA, Boydston LA, Brookshier TR, McNulty SG, Nsumu NN, Brewer BP, Blackmore K. Iron metabolism mutant hbd mice have a deletion in Sec1511, which has homology to a yeast gene for vesicle docking. *Genomics.* 2005; 86:668–673. [PubMed: 16289749]

- Wingert RA, Brownlie A, Galloway JL, Dooley K, Fraenkel P, Axe JL, Davidson AJ, Barut B, Noriega L, Sheng X, et al. The chianti zebrafish mutant provides a model for erythroid-specific disruption of transferrin receptor 1. *Development*. 2004; 131:6225–6235. [PubMed: 15563524]
- Wong P, Hattangadi SM, Cheng AW, Frampton GM, Young RA, Lodish HF. Gene induction and repression during terminal erythropoiesis are mediated by distinct epigenetic changes. *Blood*. 2011; 118:e128–138. [PubMed: 21860024]
- Xu Y, Hortsman H, Seet L, Wong SH, Hong W. SNX3 regulates endosomal function through its PX-domain-mediated interaction with PtdIns(3)P. *Nat Cell Biol*. 2001; 3:658–666. [PubMed: 11433298]
- Yoshimori T, Yamamoto A, Moriyama Y, Futai M, Tashiro Y. Bafilomycin A1, a specific inhibitor of vacuolar-type H(+)-ATPase, inhibits acidification and protein degradation in lysosomes of cultured cells. *J Biol Chem*. 1991; 266:17707–17712. [PubMed: 1832676]
- Yu M, Riva L, Xie H, Schindler Y, Moran TB, Cheng Y, Yu D, Hardison R, Weiss MJ, Orkin SH, et al. Insights into GATA-1-mediated gene activation versus repression via genome-wide chromatin occupancy analysis. *Mol Cell*. 2009; 36:682–695. [PubMed: 19941827]
- Zhang AS, Sheftel AD, Ponka P. The anemia of “haemoglobin-deficit” (hbd/hbd) mice is caused by a defect in transferrin cycling. *Exp Hematol*. 2006; 34:593–598. [PubMed: 16647565]
- Zhang J, Socolovsky M, Gross AW, Lodish HF. Role of Ras signaling in erythroid differentiation of mouse fetal liver cells: functional analysis by a flow cytometry-based novel culture system. *Blood*. 2003; 102:3938–3946. [PubMed: 12907435]
- Zhang P, Wu Y, Belenkaya TY, Lin X. SNX3 controls Wingless/Wnt secretion through regulating retromer-dependent recycling of Wntless. *Cell Res*. 2011; 21:1677–1690. [PubMed: 22041890]



**HIGHLIGHTS**

1. *Snx3* is highly expressed in vertebrate hematopoietic tissues.
2. Silencing of *Snx3* results in anemia and hemoglobin defects in vertebrates.
3. *Snx3* and *Vps35* physically interact with Tfrc.
4. *Snx3* is required for endosomal recycling of Tf-Tfrc complex.

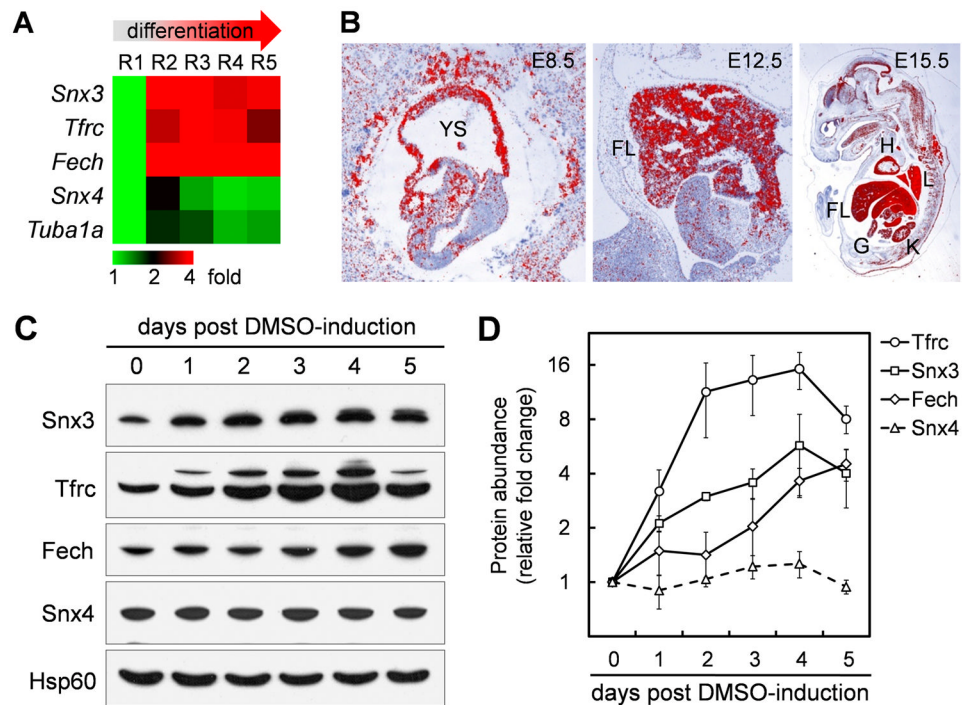


### Figure 1. *Snx3* is highly expressed in erythroid tissues

(A) *Snx3* is upregulated during the erythroid maturation of mouse fetal liver cells. The schematic heat map shows the results of an mRNA sequencing experiment on *Snx3* and control genes in the five erythroid sub-populations sorted from mouse fetal liver at E12–16 (Wong et al., 2011). The arrow on the top indicates the process of red cell maturation with R1 population representing primitive progenitor cells and proerythroblasts and R5 population representing late orthochromatophilic erythroblasts and reticulocytes (Zhang et al., 2003). (B) *Snx3* transcripts are enriched in mouse hematopoietic tissues. *In situ* hybridization revealed robust expression of *Snx3* in the yolk sac (YS) blood islands at E8.5 and fetal liver (FL) at E12.5 and E15.5. At E15.5, *Snx3* is also expressed in heart (H), lung (L), kidney (K), and gut (G). (C) *Snx3* is up-regulated during the chemically induced differentiation of MEL cells. MEL cells were chemically differentiated with DMSO for the indicated number of days. The expression of *Snx3* and control genes was detected by western in total cell lysates. (D) Quantification of the immunoblots from panel (C). Error bars represent SEM from two biological replicates.

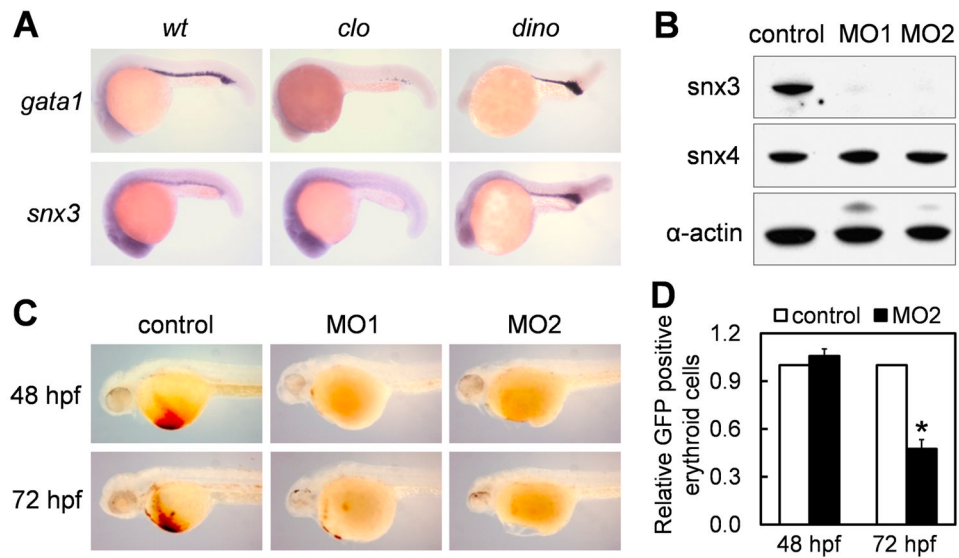


**Figure 2. Snx3 is required for heme production in zebrafish embryos**

(A) Whole-mount *in situ* hybridization detects expression of *gata1* and *snx3* in the blood island ICM in zebrafish embryos at 24 hpf. The ICM staining is absent in *cloche* mutants and is expanded in *dino* mutants. (B) Western analysis confirms efficient silencing of *snx3* by a translation-blocking morpholino (MO1) and a pre-mRNA splice-blocking morpholino (MO2). The expression of *snx4* and  $\alpha$ -actin control proteins was unaffected. (C) Injections of MOs against *snx3* result in a profound anemia in zebrafish embryos at both 48- and 72-hpf. (D) Knockdown of *snx3* in *Tg(globin-LCR:eGFP)* transgenic zebrafish leads to reduced number of erythrocytes at 72 hpf, but not at 48 hpf. Error bars represent SEM from three biological replicates. \* $P < 0.001$  compared with the control morpholino.

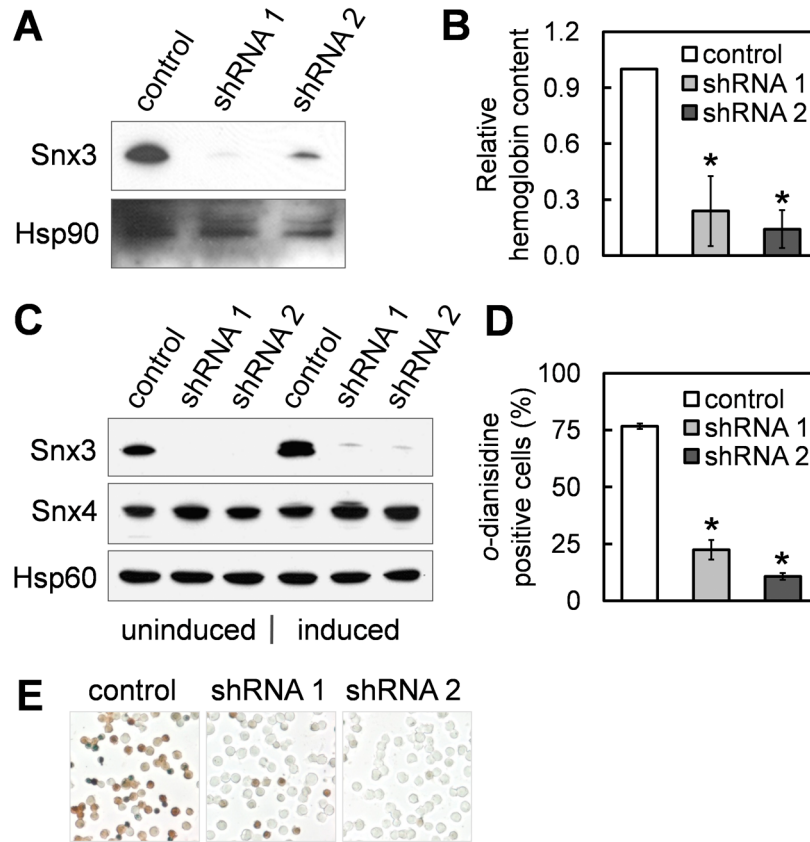


**Figure 3. Knockdown of *snx3* results in hemoglobinization defects in mouse hematopoietic cells** (A) Western analysis confirms the silencing of *Snx3* by shRNA in mouse primary fetal liver cells. (B) Silencing of *Snx3* by shRNA reduces the hemoglobin content in mouse primary fetal liver cells. Error bars represent SEM from two independent experiments. \* $P < 0.05$  compared with the control. (C) *Snx3* expression is inhibited in stable MEL clones expressing two shRNA hairpins under both undifferentiated and chemical differentiated conditions. (D) Knockdown of *Snx3* impairs hemoglobin production in MEL cells during differentiation. Error bars represent SEM from three replicates. \* $P < 0.001$  compared with the control shRNA clone. (E) Representative images of cytopsin MEL cells stained with *o*-dianisidine for hemoglobin from panel (D).

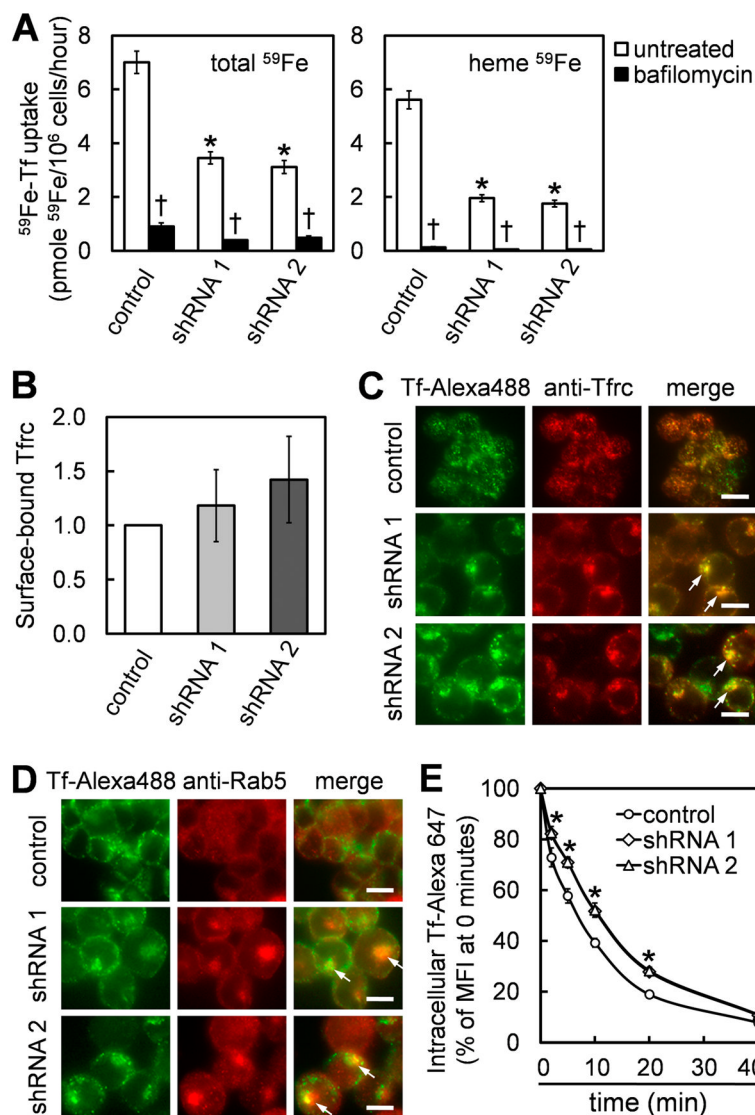


**Figure 4. *Snx3* is essential for the uptake of Tf bound iron in differentiated MEL cells**  
 (A) *Snx3*-silenced MEL cells exhibit reduced uptake of Tf bound iron. The cellular uptake of <sup>59</sup>Fe-Tf and the incorporation of imported <sup>59</sup>Fe into heme are both affected. Treatment with bafilomycin, an inhibitor of the vacuolar type H(+)-ATPase, reduced the uptake of <sup>59</sup>Fe-Tf to a similar extent in the control and *Snx3*-silenced cells. Error bars represent SEM from three replicates. \**P* < 0.05 compared with the control shRNA clone; †*P* < 0.01 compared with the untreated cells. (B) The levels of surface-bound Tfrc are not affected in *Snx3*-silenced MEL clones. FITC-labeled anti-CD71 antibody was incubated with the MEL cells and the fluorescence was measured by flow cytometry. Error bars represent SEM from three replicates. (C and D) Internalized Tf-Tfrc complex accumulates as large intracellular clusters in early endosomal compartments (arrows) in *Snx3*-silenced MEL clones. Scale bars, 10 μm. (E) Pulse-chase study using Tf-Alexa 647 reveals delayed release of internalized Tf in *Snx3*-silenced cells. The mean fluorescence intensities (MFI) of intracellular Tf-Alexa 647 are presented as percent signal relative to time 0. Error bars represent SEM from two replicates within a single experiment. \**P* < 0.01 between both *Snx3*-silenced clones and the control shRNA clone.



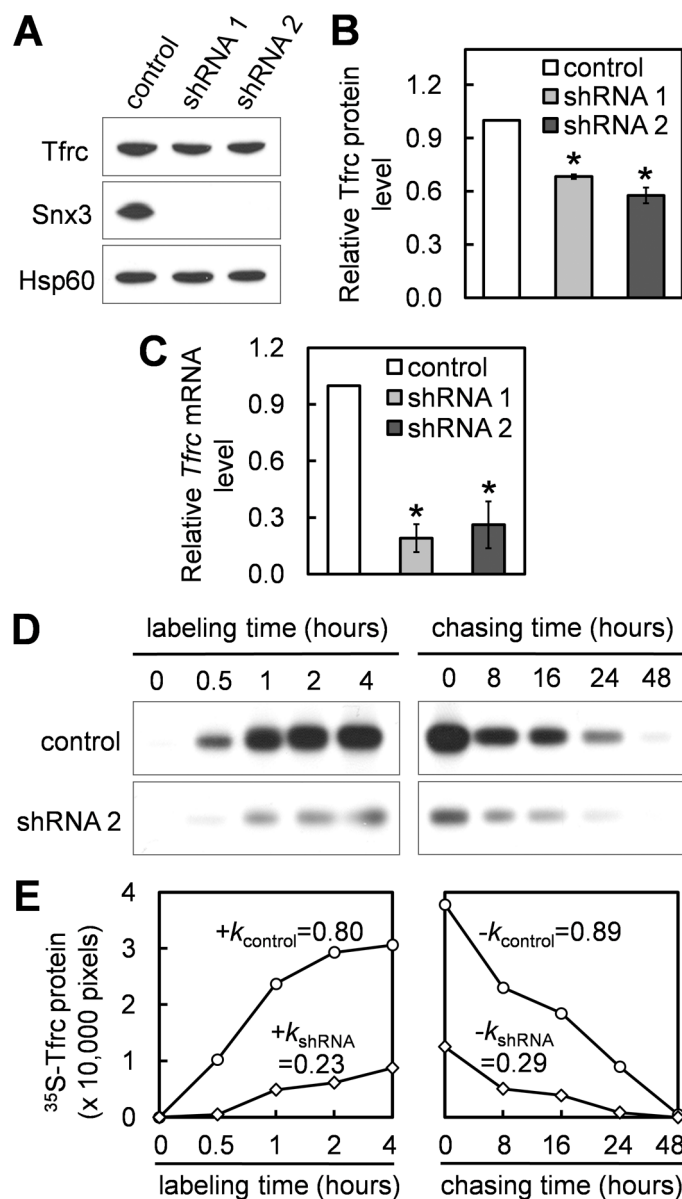


**Figure 5. Silencing of *Snx3* reduced the rates of both synthesis and degradation of Tfrc** (A) The steady-state level of total Tfrc protein is moderately reduced in *Snx3*-silenced MEL cells. (B) Quantification of the immunoblots from panel (A). Error bars represent SEM from two biological replicates. \* $P < 0.05$  compared with the control shRNA clone. (C) qRT-PCR analysis shows reduced amounts of *Tfrc* mRNA in *Snx3*-silenced MEL cells. Error bars represent SEM from two independent experiments. \* $P < 0.05$  compared with the control shRNA clone. (D)  $^{35}\text{S}$  pulse-chase assays demonstrate lower rates of both synthesis and degradation of Tfrc protein. (E) Quantification of autoradiographic bands of  $^{35}\text{S}$ -Tfrc from panel (D). The experiments were performed in one replicate. Linear regression models were fitted to the data, and the slopes were indicated as  $+k$  or  $-k$  for the rates of synthesis or degradation, respectively.

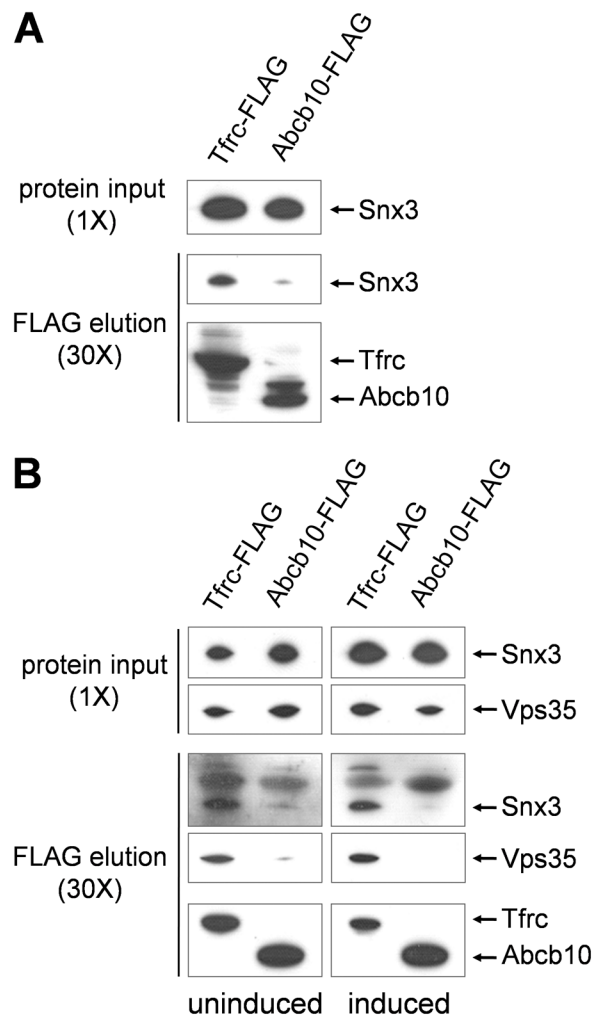


**Figure 6. Physical interactions among Snx3, Vps35, and Tfrc**

(A) Protein pull-down assays in a heterologous system indicate interactions between Snx3 and Tfrc. Cell lysates from HEK293 cells ectopically expressing *Tfrc*-FLAG or the control *Abcb10*-FLAG combined with *Snx3* were purified with anti-FLAG beads followed by western analysis. The western blots of whole cell lysates (protein input) and the binding fractions (FLAG elution, 30×) are presented. (B) Tfrc interacts with both Snx3 and Vps35 in MEL cells. MEL cells stably expressing *Tfrc*-FLAG or the control *Abcb10*-FLAG were subjected to the protein pull-down assays. The endogenous Snx3 and Vps35 copurified with Tfrc-FLAG, but not with *Abcb10*-FLAG.

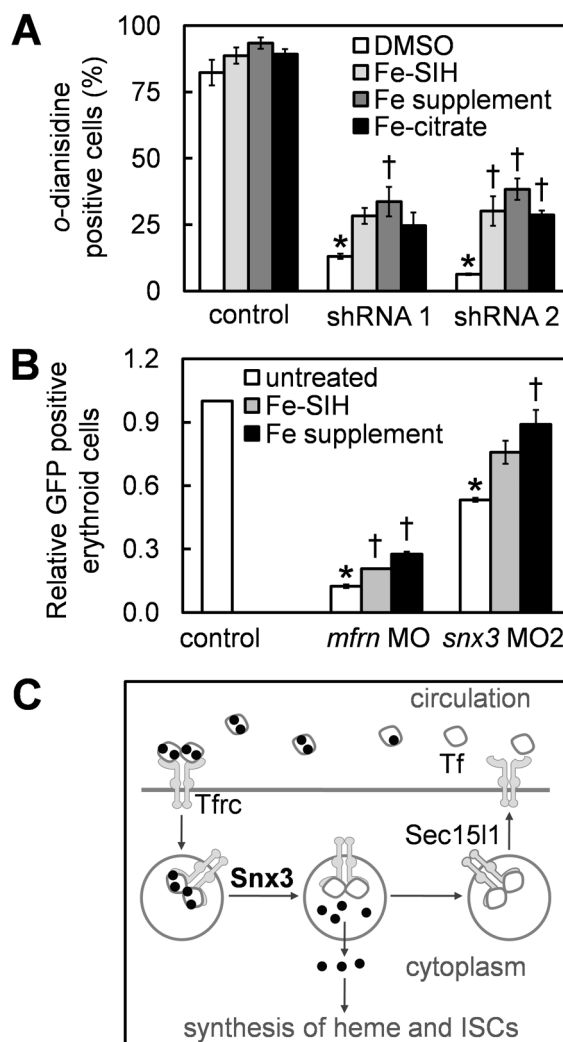


**Figure 7. Complementation of the hemoglobinization defects with non-Tf bound iron supplements**

(A) Fe-SIH, ferric citrate, and a chemically defined iron supplement increase the hemoglobin production in *Snx3*-silenced MEL cells after chemically induced differentiation. Error bars represent SEM from three independent experiments. \* $P < 0.001$  compared with the control clone; † $P < 0.05$  compared with the DMSO control within the group. (B) Fe-SIH and a chemically defined iron supplement restore the number of erythrocytes in *snx3* morphant zebrafish embryos at 72 hpf. *Mitoferrin1* (*mfrn*) is used as a positive control for iron rescue. Error bars represent SEM from two independent experiments. \* $P < 0.001$  compared with the control morpholino; † $P < 0.05$  compared with the untreated embryos. (C) The proposed role of Snx3 in Tf cycle. In early endosomes, Snx3, along with Vps35, transiently interacts with and sorts the Tf-Tfrc complex into recycling endosomes. Sec151 regulates the trafficking of Tf-Tfrc complex from recycling endosomes to cell surface. ISCs, iron sulfur clusters.